Proceedings of the
4th JSME-KSME Thermal Engineering Conference
October 1-6, 2000, Kobe, Japan

D309

CONTROL OF SIZE, MORPHOLOGY AND PHASE OF NANO PARTICLES USING CO_2 LASER IRRADIATION

Mansoo Choi and Donggeun Lee

School of Mechanical and Aerospace Engineering, Seoul National University, Seoul 151-742, Korea, Also at
National CRI Center for Nano Particle Control, Institute of Advanced Machinery and Design
E-mail) mchoi@plaza.snu.ac.kr

ABSTRACT Nano crystalline or non-crystalline particles have been widely used in various industrial area, such as ceramics, catalysis, electronics, metallurgy and optic device. In all applications, synthesizing the particles as small as possible and controlling the crystalline phase according to its purpose are necessary for the enhancement of materials properties. In some cases, non-agglomerated particles may be necessary for solving the packing problems. This motivates our attempt of controlling size, morphology, phase of nano titania and silica particles. If one can enhance sintering rate of small aggregates independently of collision rate, one may expect that original aggregates can be changed into volume equivalent spheres and thereby the decrease of collision frequency due to the change leads to much smaller rate of growth of the particles. Rapid heating and cooling of nanoparticles can occur when nanoparticles are irradiated by high power laser beam and this has been also utilized to control the crystalline phase of nanoparticles. This is the basic idea of our control strategy.

1.INTRODUCTION

The morphology and size of particles are determined by the competition between collision and coalescence of particles [1]. The formation of aggregates is due to faster collision of particles than coalescence. The electrical field had been applied in a particle generating flame to successfully control the size of primary particles and aggregates, however, the formation of aggregates could not be avoided [2,3,4]. The present method relies on controlling the characteristic time for coalescence of nanoparticles by irradiation of CO_2 laser beam on the early stage aggregates formed during flame synthesis that has been considered as the most effective way to produce high concentration nanoparticles [5].

The coalescence characteristic time depends strongly on particle temperature following the exponential decay [6] while the collision characteristic time of nanoparticles decays according to $T_p^{-1/2}$ [1]. Therefore, the coalescence characteristic time can be controlled nearly independently of Brownian collision by heating aggregates rapidly. Early stage aggregates formed in a flame are irradiated by a high power CW CO_2 laser beam to rapidly coalesce and become spherical particles. Since spherical particles have much smaller collision cross-sections than volume equivalent aggregates [1,5], much slower growth of nanoparticles can be achieved.

A coflow oxy-hydrogen diffusion flame burner was used for hydrolysis of $SiCl_4$ and $TiCl_4$ to produce silica and titania particles, respectively. TEM image analysis with local thermophoretic sampling and a light scattering technique were utilized to study the effect of laser irradiation in a flame on the change of size and morphology of the particles. Both the measurements of the scattered intensity with Ar-ion laser light and observation of TEM photographs reveals that the present control is successful. X-ray Diffraction was also used for determining the crystallinity of titania.

2.EXPERIMENTAL

A laminar diffusion flame burner is used for synthesis of the particles. Figure 1 shows the experimental setup which consists of a burner, two laser optical systems for particle heating and light scattering measurement, and a local thermophoretic sampling device. The burner is composed of six concentric stainless steel tubes. The carrier gas passed through a bubbler containing $SiCl_4$ liquid is injected through the center nozzle of the burner, and shield gas N_2 is injected through eight circumferential holes adjacent to the center nozzle to prevent deposition of formed particles on the nozzle surface. Hydrogen and oxygen are injected through the next two concentric annuli in that order. Dry air flows through the outer tube (25.4mm ID and 53mm OD) which contains a honeycomb with 100 openings cm^{-2} and three fine meshes in order to stabilize the flame.

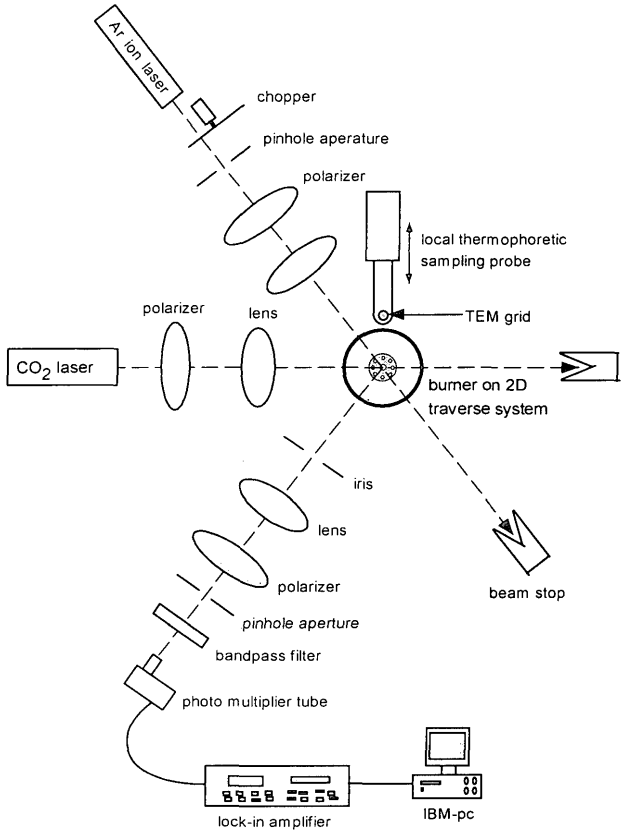

Fig. 1 Experimental setup

A bubbler containing $SiCl_4$ liquid is maintained at 26°C for all experiments. The carrier gas N_2 passed through the bubbler is nearly saturated with $SiCl_4$ vapor in the present study. Therefore, maintaining the constant velocity of gas injected through the center nozzle for different carrier gas flow rates would require the additional gas (N_2) dilution before entering the center nozzle. In contrast to the case of $SiCl_4$, since the vapor pressure of $TiCl_4$ (Aldrich, 99.9%) is much lower than that of $SiCl_4$, the bubbler containing $TiCl_4$ is maintained at relatively high temperature above 40°C.

An industrial 2800W continuous wave (CW) CO_2 laser, radiating at a wavelength of 10.6μm was used to rapidly heat up particles.

The laser beam was partially focused with a ZnSe lens (focal length, 150mm) to a beam of 3.6mm in diameter that covered the orthogonal upward stream of chemical mixture and oxy-hydrogen flame-generated silica particles at the height of h_L from the burner surface. CO_2 laser powers used in this study ranged from 250 to 2500W.

A 0.5W Ar-ion laser was employed as a light source for light scattering measurements. The beam chopped at 1200Hz was focused into the test region with a 500mm focal length lens to provide a beam waist of 0.2mm in the test region. The scattered light at 75° angle was focused into the entrance pinhole aperture of a photo multiplier tube (PMT, Hamamatsu R928). The entrance pinhole aperture and the size of the laser beam waist defined the measuring volume.

Signals from the PMT were fed into a lock-in amplifier (Stanford Research Systems Inc., SR830) for amplifying only the chopped light signals and canceling other noise components. The Ar-ion laser beam travels at the height of h_p located 5mm higher than the CO_2 laser irradiation height (h_L). The reason is that the local thermophoretic sampling for examining size and morphology could not be made at the position where CO_2 laser beam was irradiated. Ar-ion light scattering measurement and local sampling should be done at the same position (h_p).

Sizes and shapes of silica particles were measured by TEM image processing after the local sampling of particles was made. To compare the result of light scattering with that of the sampling, particles in the same volume of light scattering should be captured, correspondingly, a local sampling is necessary. The local sampling device [7,8] consists of a sampling probe holding a TEM grid, a shield covering the TEM grid, two air cylinders and three timers to control the insertion times of the probe and the shield independently. The shield covers the probe to prevent deposition of particles on the grid when the probe was inserted into the desired local point in a flame and pulled out of the flame. The sampling area of the grid is confined by 1.5mm diameter hole and exposed to flames for about 70 ms.

3. Result and Discussion

To find out morphological changes of particles in an oxy-hydrogen flame, particles were locally captured at various heights along the centerline in the absence of CO_2 laser irradiation and the corresponding TEM photos were shown in Fig. 2. Figure 2 obviously shows the fast evolution of silica particles from the forming stage to fully-sintered spheres along the centerline of the flame.

To confirm the above-mentioned effects of laser irradiation, CO_2 laser beam with various powers were irradiated at h_L equal to 6mm and 12mm above the burner surface and particles were captured simultaneously at h_p equal to 11mm and 17mm, respectively. Figures 3 and 4 show the corresponding TEM photos, respectively, for carrier gas flow rate of 50 cc/min. Flow rates of H_2, O_2, dilution gas N_2, shield gas N_2 and dry air are 2.5 l/min, 5.0 l/min, 150 cc/min, 400 cc/min and 70 l/min, respectively.

As shown in Fig. 3 that corresponds to the low irradiation height, the particle-generation effect is obvious as CO_2 laser power increases; for example, from clear difference between cases of P = 0 and 760W. In addition, primary particle size was found to increase and the fraction of nearly-unagglomerated particles tends to increase with increasing CO_2 laser power (see Fig. 3(c)). The latter part would be attributed to enhanced particle generation and co-existing sintering effect. The intensity of Ar ion laser light scattering has been shown to increase as CO_2 laser powers increase (not shown here).

Figure 4 shows the evolution of morphology of particles irradiated at h_L = 12mm by CO_2 laser beam and captured at h_p = 17mm. From Figs. 2(a) and 2(b), it is easily known that small aggregates would exist in the region from z = 12mm to z = 14mm without CO_2 laser irradiation.

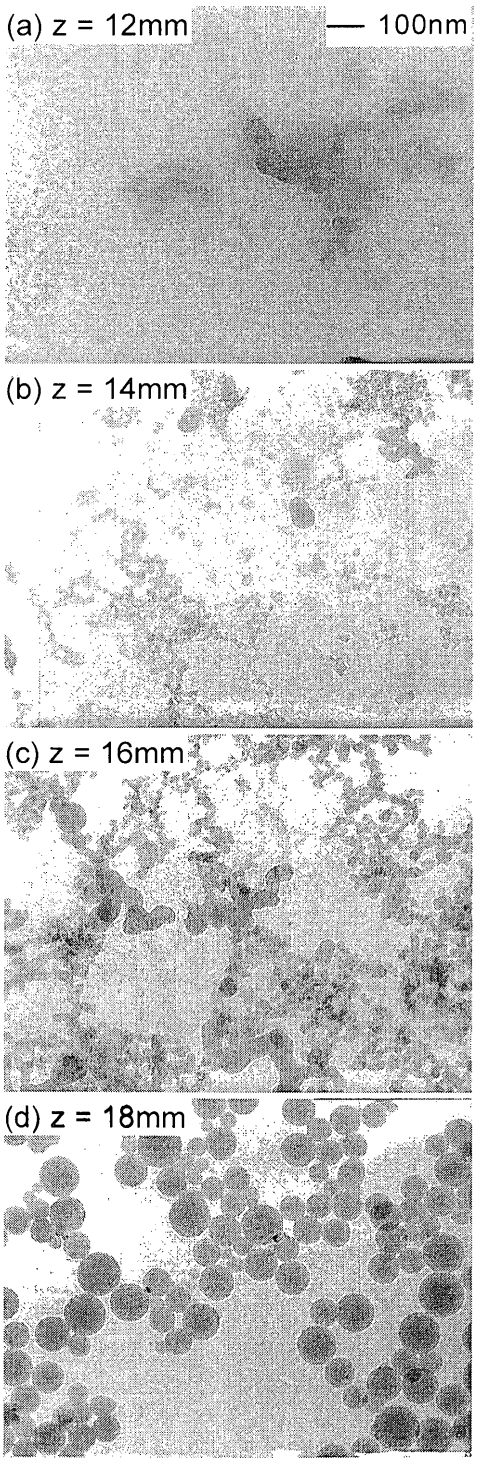

Fig. 2. TEM images of SiO_2 particles at different heights without CO_2 laser irradiation.

It is also noted that the radius of CO_2 laser beam is 1.8mm, therefore, the laser beam irradiates small aggregates. When the laser irradiates at this intermediate height, the originally existing aggregates in a flame can be heated up to high temperatures that may be less than the evaporation temperature, but high enough to enhance sintering.

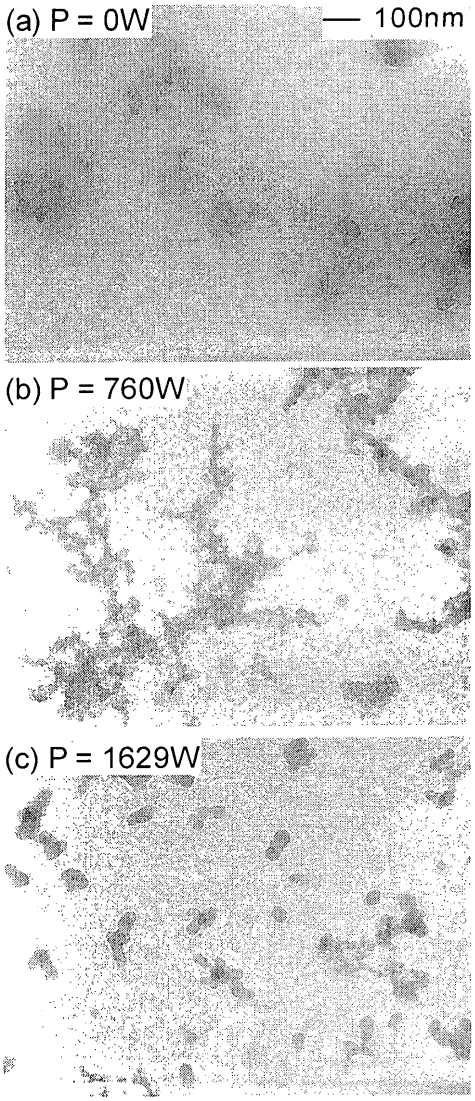

Fig. 3. TEM images of SiO_2 particles captured at 11mm with increasing CO_2 laser powers; h_L=6mm.

Thus, aggregates could be converted into more sphere-like particles. Consequently, the size of particles captured 5mm higher can be reduced maintaining spherical shape due to much lower collisional cross section of spheres than that of the volume-equivalent aggregates as described in Introduction. As the laser power increases, the average diameter of spherical particles evidently decreases to about 60% of the size of the case without CO_2 laser irradiation (about 20% in volume) as can be seen in Fig. 4. Thus, the control strategy adopted in the present study, which is the control of the sintering characteristic time, seems to be promising for the flame synthesis of more spherical and smaller particles. Beyond the laser power of 1170W, aggregates composed of a few nanometer sized primary particles also appeared together with about 40nm spherical particles. The higher the laser power, the more aggregates appeared.

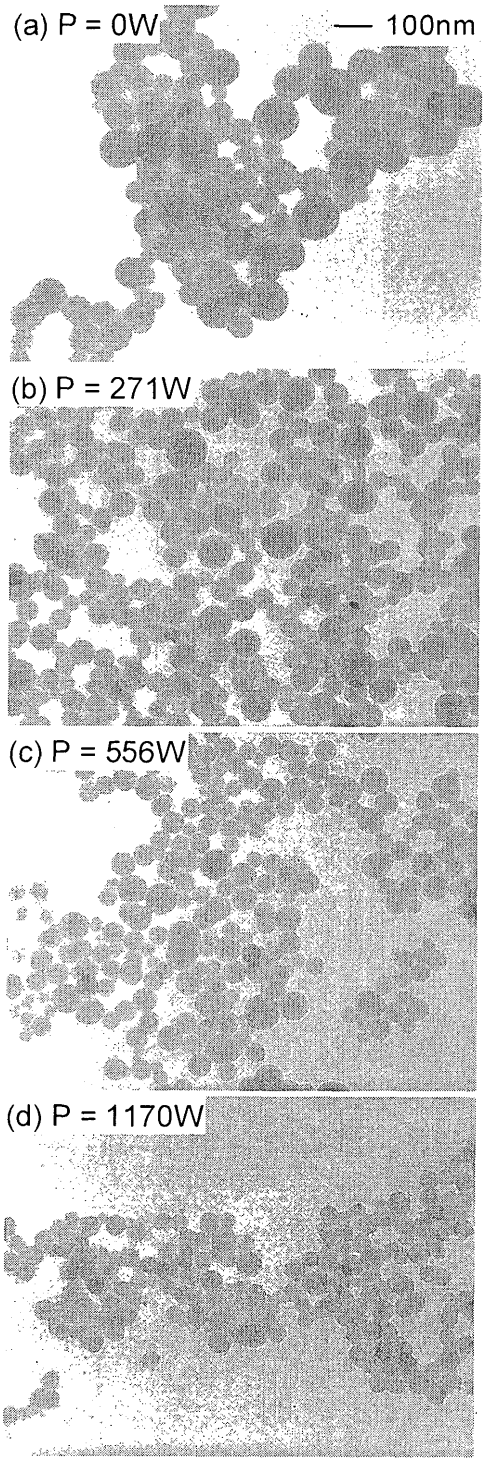

Fig. 4. TEM images of SiO_2 particles captured at 17mm with increasing CO_2 laser powers; h_L=12mm

For extremely high power such as 2500W, all observed particles were composed of only aggregates (not shown), which could be explained as a result of evaporation and recondensation. Both mean diameter (d_{avg}) and standard deviation (STD) of particles from TEM image analysis decrease monotonically with increasing CO_2 laser power.

All statistical data were obtained by averaging 2000 – 3000 particles each case and the sensitivity of sample numbers of particles for a proper averaging was also checked. Also, the dispersion α defined by STD/d_{avg} decreases up to approximately 0.2. This indicates the size distribution to become more uniform one. Cai et al. [9] noted that nearly mono-disperse distribution could be assumed when Fuch's criterion α was smaller than 0.2.

We also applied the present method to control the growth of crystalline nanoparticles of titania using $TiCl_4$ precursor. Figure 5 shows the changes of size and morphology of titania particles captured at 16mm without or with CO_2 laser beam irradiated at 13mm. As CO_2 laser powers increase, coalescence is clearly shown to be enhanced and original aggregates finally become fully sintered spherical particles (Fig. 5(c)). The magnified TEM image indicates that seemingly agglomerate particles in Fig. 5(c) turn out to be just a multiple deposition of isolated sphere particles on TEM grid. As laser power increases, projected area equivalent diameters significantly decrease (projected area equivalent diameters: 166nm for P=0W and 29nm for P=1665W). Furthermore, it is estimated that average volume of particles also decreases substantially by about 30 times.

The controllability of crystalline phase has also been investigated. Figure 6 shows X-ray diffraction profiles of titania particles collected at 65mm for different laser powers when the laser beam is irradiated at 25mm. In Fig. 6, A and R denote anatase and rutile, respectively. It is interesting that rutile contents decrease monotonically with the increase of laser power. For sufficiently high laser powers, rutile peaks completely disappear. This is a surprising result since rutile phase is well known to be more stable than anatase phase when particle size exceeds 14nm [10]. Therefore, previous researchers [11,12] reported the transformation of anatase phase to rutile as particle temperature increased and we could not find any studies on the transformation from rutile to anatase phase. In the absence of CO_2 laser irradiation, rutile weight percent increases monotonically with flame height; 0% at 13 mm, 2.6% at 15mm, 6.9% at 20mm, 10.3% at 25 mm, 13.3 % at 40 mm and 16.6% at 65 mm. This is consistent with previous studies. But, the present study reveals that the irradiation of CO_2 laser beam can alter the phase from rutile to anatase. For example, 17% rutile weight percent of particles at 65 mm without CO_2 laser irradiation is now changed to 0 %, i.e., pure anatase particles when CO_2 laser beam is irradiated at 25mm with P=326W. This could be explained by the possible occurrence of melting of titania particles due to the irradiation of laser beam and subsequent re-crystallization after passing the laser irradiation zone (beam diameter: 3.3 mm). Extremely fast cooling of melted particles can be easily expected because of very small size of particles. Since sufficient time is needed for atomic rearrangement leading to more compact and stable rutile phase, the initial solid phase from melted titania after a fast cooling might prefer anatase phase. The metastable anatase could be re-crystallized preferably from solution since the critical nucleus radius of anatase would be smaller than that of rutile [13].

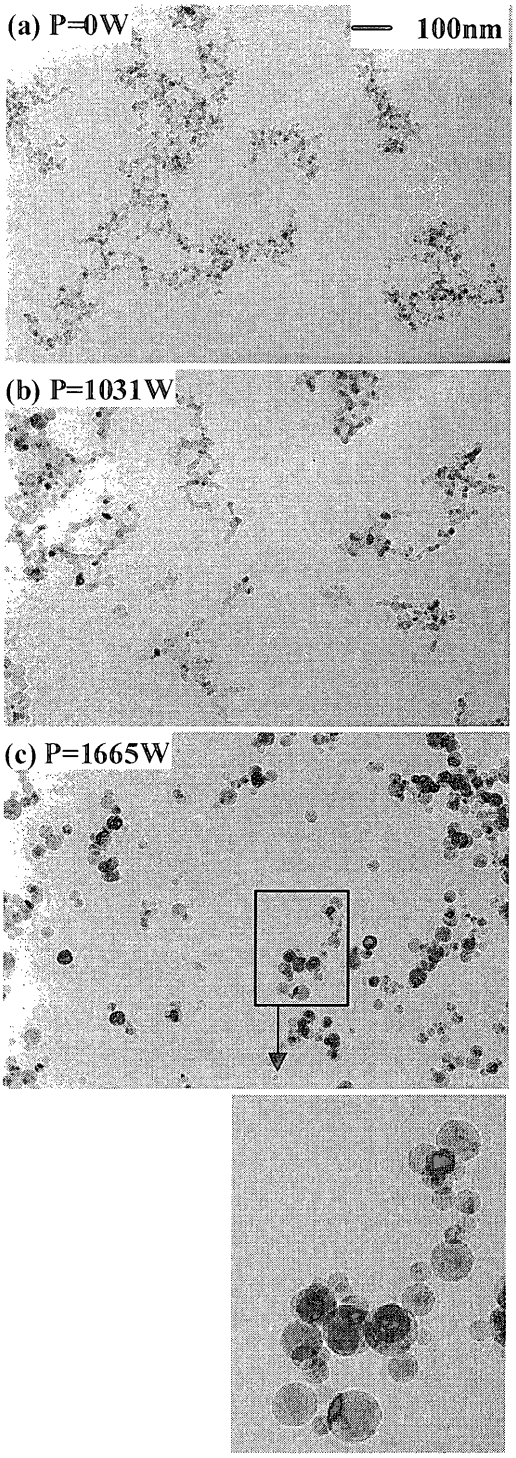

Fig. 5. TEM images of TiO_2 particles captured at 16mm with increasing CO_2 laser powers under Condition B; h_L=13mm

4. Conclusions

In summary, the control of the size, morphology and crystalline phase of nanoparticles has been done successfully by irradiating laser beam on the early formed

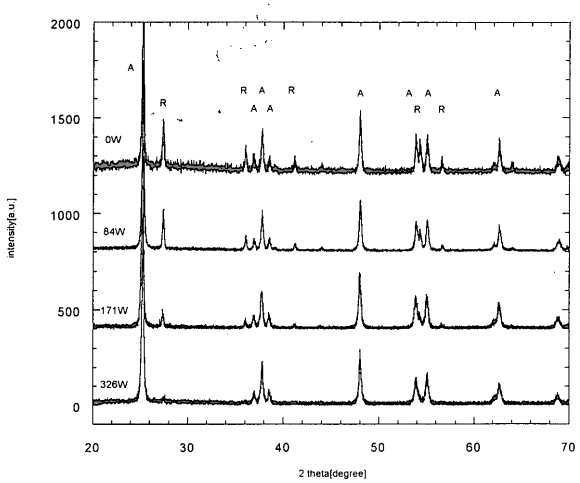

Fig. 6. Variations of X-ray diffraction profiles with increasing CO_2 laser powers; h_L=25mm, h_p=65mm.

aggregates in flames. This method seems to be applicable to the synthesis of other single or multicomponent nanoparticles with controlled structure and may be extended to other processes as well as flame synthesis.

References

1. Windeler, R.S., Friedlander, S.K. and Lehtinen, K.E.J., Production of nanometer sized metal oxide particles by gas phase reaction in a free jet I and II, Aerosol Sci. and Technol., Vol.27 (1997), pp.174 and 191
2. Vemury, S. and Pratsinis, S.E., Corona-assisted flame synthesis of ultrafine titania particles, Appl. Phys. Lett. Vol.66 (1995), pp.3275
3. Vemury, S. and Pratsinis, S.E., Charging and coagulation during flame synthesis of silica, J. Aerosol. Sci., Vol.27 (1996), 951
4. Vemury, S., Kibbey, L. and Pratsinis, S.E. Electrically controlled flame synthesis of nanophase TiO_2, SiO_2, and SnO_2 powders, J. Materials Research,Vol.12 (1997), pp.1031
5. Pratsinis, S.E., Flame aerosol synthesis of ceramic powders, Prog. Energy Combust. Sci., Vol.24 (1998), pp.197
6. Kingery, W.D., Bowen, H.K. and Uhlmann, D.R., Introduction to Ceramics, (1976), Wiley, New York
7. Cho, J. and Choi, M., Determination of number density, size and morphology of aggregates in coflow diffusion flame using light scattering and local sampling, J. Aerosol Sci., in press. (2000)
8. Lee, D. and Choi, M., Control of size and morphology of nano particles using CO_2 laser during flame synthesis, J. Aerosol Sci., in press. (2000)
9. Cai, H., Chaudhary, N., Lee, J., Becker, M.F., Brock, J.R. and Keto, J.W., Generation of metal nanoparticles by laser ablation of microspheres. J. Aerosol Sci., Vol. 29(5/6) (1998), pp.627

10. Zhang, H. and Banfield, J.F., Thermodynamic analysis of phase stability of nanocrystalline titania, J. Mater. Chem., Vol.8 (1998), pp.2073-2076
11. Gribb, A.A. and Banfield, J.F., Particle size effects on transformation kinetics and phase stability in nanocrystalline TiO_2, American Mineralogist, Vol.82 (1997), pp.717-728
12. Ding, X.-Z. and Liu, X.-H., Grain size dependence of anatase-to-rutile structural transformation in gel-derived nanocrystalline titania powders, J. Materials Sci. Lett., Vol.15 (1996), pp.1789-1791
13. Gribb, A.A. and Banfield, J.F., Particle size effects on transformation kinetics and phase stability in nanocrystalline TiO_2, American Mineralogist, Vol.82(1997), pp.717-728

Acknowledgement

This work was funded by National CRI Center for Nano Particle Control supported by the Ministry of Science and Technology, Korea.